

Figure S1, Related to Figure 1. CD23⁺ LZ cells showed enrichment for a BCR signaling signature.

(A) The visualize signature score of the top 50 marker genes of day7 cluster 3 (CD23⁺) GC B cells in day 14 GC B cell dataset, calculated by VISION. Color scaled with signature score. Dashed line showed cluster 1 in day 14 dataset.

(B, C) UMAP plots of the expression of *Myc* (B) and visualize signature scores of MYC targets (C) in day 7 GC B cell dataset. Color scaled for each gene with log normalized expression level or signature score. Dashed line gated region represents cluster 2.

(D, E) UMAP plots of the expression of *Cd40* (D) and visualize signature scores of CD40 signaling (E) in day 7 GC B cell dataset. Color scaled for each gene with log normalized expression level or signature score. Dashed line gated region represents cluster 2.

(F) Visualize signature scores of hallmark mTORC1 signaling calculated by VISION in day 7 GC B cell dataset. Color scaled with signature score. Dashed line gated region represents cluster 2.

(G) Visualize signature scores of KEGG Glycolysis Gluconeogenesis pathway in day 7 GC B cell dataset (left), UMAP plots of the expression of *Hk2* (right). Color scaled for each gene with log normalized expression level or signature score. Dashed line gated region represents cluster 2.

(H) Visualize signature scores of hallmark BCR signaling pathway calculated by VISION in day 7 GC B cell dataset. Color scaled with signature score. Dashed line gated region represents cluster 3.

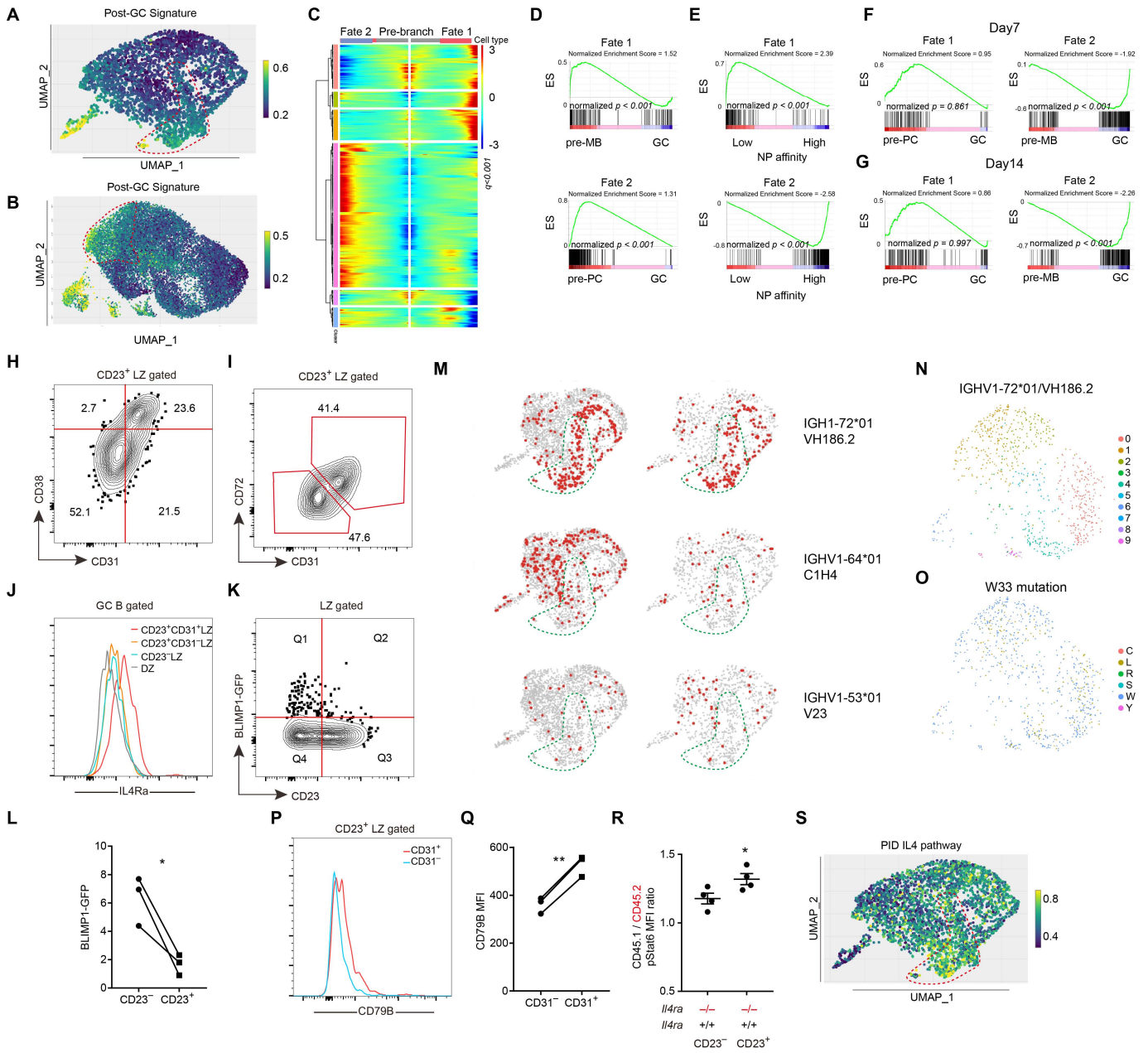


Figure S2, Related to Figure 2 and 3. Properties of CD23⁺ LZ B cells

(A, B) Visualize signature scores of post-GC (Efnb1⁺ S1pr^{low}) B cell in day 7 GC dataset (A) and day 14 GC dataset (B).

(C) Heatmap of differentially expressed genes between cell fate 1 and cell fate 2 within cluster 2 of day 14 LZ GC B cell dataset by pseudo-time analysis (all genes were listed in Table S4).

(D) GSEA analysis of differentially expressed genes from the two cell fates compared to published pre-memory B cell and pre-plasma cell RNA sequencing datasets (Ise et al., 2018; Wang et al., 2017). Enrichment profiles for cell fate 1 compared with pre-memory (upper) and cell fate 2 compared with pre-plasma cell (lower). ES presents enrichment score.

(E) GSEA analysis of differentially expressed genes from different cell fates compared to the published RNA sequencing datasets of different NP affinity GC B cells (Shinnakasu et al., 2016). Enrichment profiles for cell fate 1 compared with low-affinity (upper) and cell fate 2 compared with high-affinity (lower). ES presents enrichment score.

(F, G) GSEA analysis of differentially expressed genes from the two cell fates in day 7 (F) and day14 (G) datasets compared to published pre-plasma B cell and pre-memory cell RNA sequencing datasets (Ise et al., 2018; Wang et al., 2017). Enrichment profiles for cell fate 1 compared with pre-plasma (left) and cell fate 2 compared with pre-memory B cell (right). ES presents enrichment score.

(H, I) Representative FACS profile displaying gates between CD31 and CD38 (H), or CD31 and CD72 (I) in CD23⁺ LZ GC B cells. Data represent three independent experiments, with at least three mice per experiment.

(J) Representative histograms of IL4Ra in DZ (B220⁺ CD95^{hi} GL7^{hi} CXCR4^{hi} CD86^{lo}), CD23⁻ LZ (B220⁺ CD95^{hi} GL7^{hi} CXCR4^{lo} CD86^{hi}), CD31⁻CD23⁺ LZ and CD31⁺CD23⁺ LZ

GC B cells 12-14 days after immunization. Data represent three independent experiments, with at least three mice per experiment.

(K, L) *Blimp1*^{Gfp/+} reporter mice were immunized with NP-haptenated antigen. (K) Representative FACS profile displaying gates between CD23 and BLIMP1 in LZ GC B cells. (L) Percentages of BLIMP1⁺ cells in CD23⁻ and CD23⁺ LZ GC B cells on day 13 after immunization. Each symbol represents one mouse, and each line represents the same mouse. * $P < 0.05$.

(M) The usage of different NP specific heavy chain gene in each cluster of two day 7 GC B samples.

(N) The usage of IGHV1-72*01 in each cluster in day 14 dataset.

(O) Distribution of IGHV1-72*01 W33L mutation in each cluster in day 14 dataset.

(P, Q) Representative histograms (P) and MFI (Q) of CD79b in CD31⁺ or CD31⁻ CD23⁺LZ GC B cells. Each symbol represents one mouse, and each line represents the same mouse. One of two experiments with similar result is shown. ** $P < 0.01$.

(R) Geometric mean fluorescence intensity (MFI) of pStat6 in CD23⁻ or CD23⁺ *Ii4ra*^{+/+} GC B cells relative to the MFI of *Ii4ra*^{-/-} cells of the same type in CD45.1 *Ii4ra*^{+/+} / CD45.2 *Ii4ra*^{-/-} mixed BM chimeras. * $P < 0.05$.

(S) Visualize signature score of PID IL4 pathway calculated by VISION in day 7 GC B cell dataset. Color scaled with signature score.

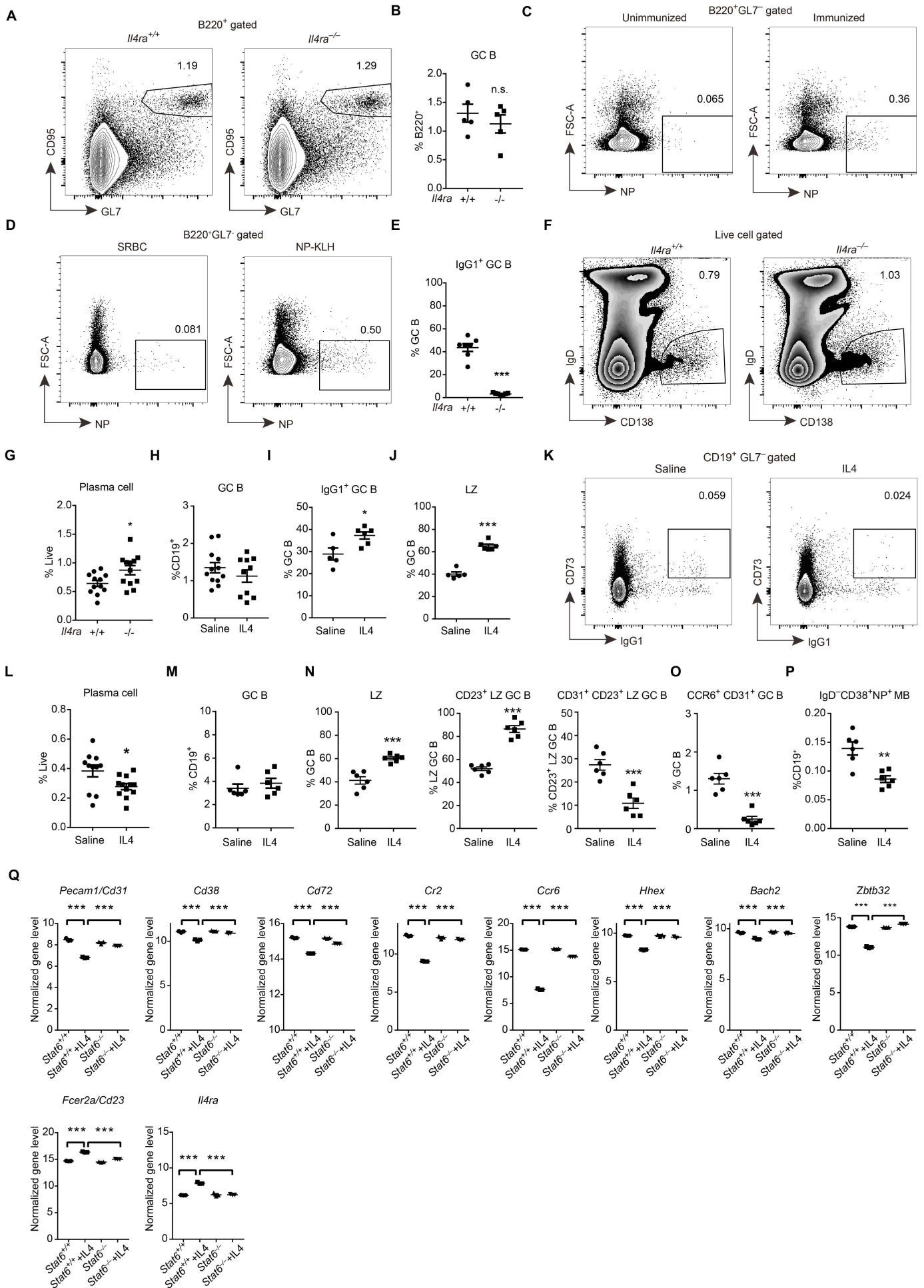


Figure S3, Related to Figure 4. Influence of IL4RA signaling on GC outputs

(A, B) Representative FACS profiles (A) and frequencies mean \pm SEM) (B) of CD95^{hi} GL7^{hi} GC B cells in B220⁺ B cells 13 days after immunization in mice with indicated genotypes. Each symbol represents one mouse. One of two experiments with similar results is shown. n.s., not significant.

(C, D) Representative FACS profiles of NP⁺ memory B cells in B220⁺GL7⁻ B cells in unimmunized (C) or NP-haptenated antigen immunized (C, D) or SRBC immunized mice (D).

(E) Frequency (mean \pm SEM) of IgG1⁺ cells in GC B cells 13 days after immunization in mice with indicated genotypes.

(F, G) Representative FACS profiles (F) and frequencies (mean \pm SEM) (G) of IgD^{low} CD138^{hi} plasma cells in splenocytes 13 days after immunization in mice with indicated genotypes. Each symbol represents one mouse. Data are pooled from three independent experiments. * P <0.05.

(H-L) Immunized mice received saline or IL4- α IL4 treatment. (H-J) Frequencies (mean \pm SEM) of CD95^{hi} GL7^{hi} GC B cells in CD19⁺ B cells (H), IgG1⁺ cells in GC B cells (I), and LZ cells in GC B cells (J). Each symbol represents one mouse. One of three experiments with similar results is shown. (K) Representative FACS profiles of IgG1⁺ CD73⁺ in CD19⁺GL7⁻ B cells in mice with indicated treatment. (L) Frequencies (mean \pm SEM) of IgD^{low} CD138^{hi} plasma cells in splenocytes in mice with indicated treatment. Each symbol represents one mouse. (I, J) One of three experiments with similar results is shown. (H, L) Data are pooled from three independent experiments. * P <0.05, *** P <0.001.

(M-P) NP-KLH immunized *Aicda*^{+/+} and *Aicda*^{-/-} BM chimeric mice received saline or IL4- α IL4 treatment. (M) Frequencies (mean \pm SEM) of CD95^{hi} GL7^{hi} GC B cells in CD19⁺

B cells. (N-P) Frequencies (mean \pm SEM) of LZ cells in GC B cells (N left), CD23⁺ cells in LZ GC B cells (N middle), CD31⁺ cells in CD23⁺ LZ GC B cells (N right), CD31⁺CCR6⁺ cells in GC B cells (O), and IgD⁻CD38⁺NP⁺ memory B cells in CD19⁺ B cells (P). Each symbol represents one mouse. Data are pooled from two independent experiments. ** $P < 0.01$, *** $P < 0.001$.

(Q) Normalized expression of different gene in *Stat6*^{+/+} and *Stat6*^{-/-} primary B cell after IL4 stimulation. Data are from (Mokada-Gopal et al., 2017). *** $P < 0.001$ by one-way ANOVA with Sidak multiple comparisons test.

A

$$\text{Competency} = \frac{\text{Target pop. CD45.2/CD45.1}}{\text{Parent pop. CD45.2/CD45.1}}$$

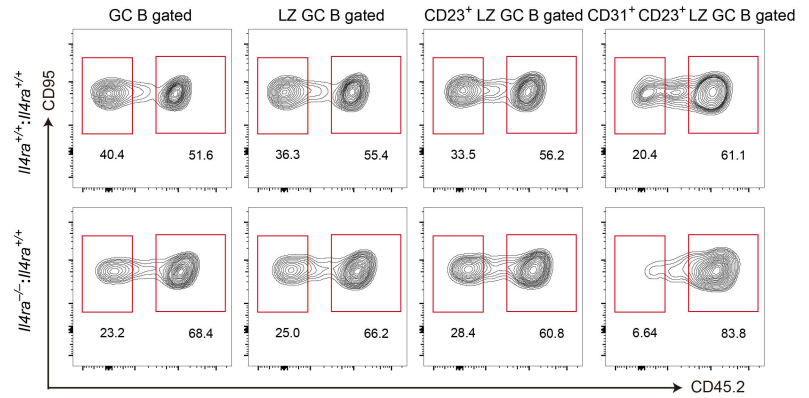
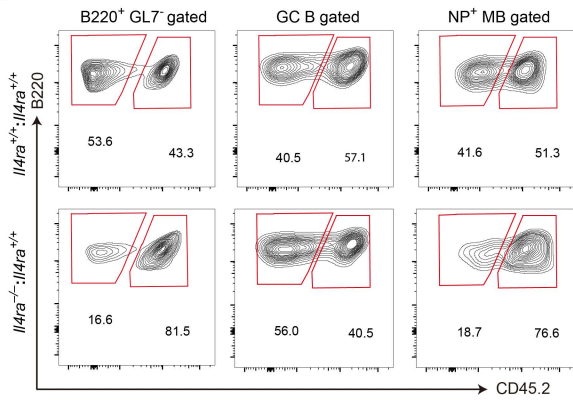
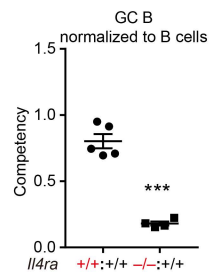
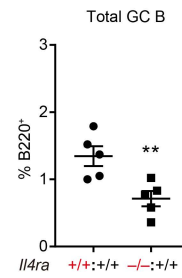
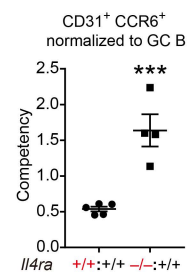
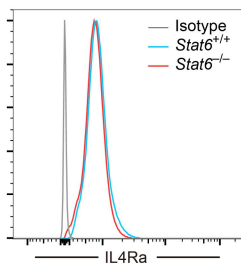
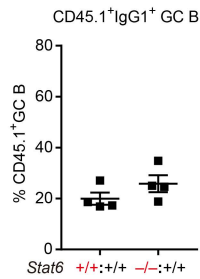
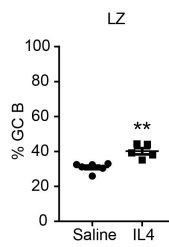
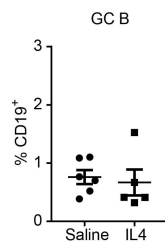
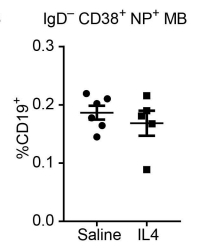
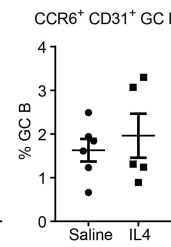
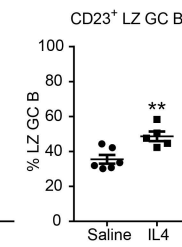
B**C****D****E****F****G****H****I****J**

Figure S4, Related to Figure 5. IL4RA and STAT6 are intrinsically required for restraining pre-memory B cell development

(A-C) Equation for calculating competitive competencies (A) and representative FACS profiles show gating strategies (B, C) for analysis of the indicated types of mixed BM chimeras.

(D, F) Competency values (mean \pm SEM) of GC B cell (D) and CD31⁺ CCR6⁺ (F) GC B cell compartment.

(E) Frequencies (mean \pm SEM) of total GC B cells.

(G) Representative histograms of IL4RA in B220⁺ FO B cells in *Stat6*^{+/+} and *Stat6*^{-/-} mice.

(H) Frequencies (mean \pm SEM) of CD45.1⁺IgG1⁺ cell in CD45.1⁺ GC B cells.

(I, J) Immunized *Stat6*^{-/-} mice received IL4- α IL4 complex or saline intravenously once per day on day 11, 12, 13 post immunization and were analyzed on day 14. (I) Frequencies (mean \pm SEM) of GC B cells in CD19⁺ B cells (I left) and LZ cells in GC B cells (I right).

(J) Frequencies (mean \pm SEM) of CD23⁺ cells in LZ GC B cells (J left), CD31⁺CCR6⁺ cells in GC B cells (J middle), and IgD⁻ CD38⁺NP⁺ memory B cells in CD19⁺ B cells (J left). Each symbol represents one mouse. One of two experiments with similar result is shown. ** $P < 0.01$.

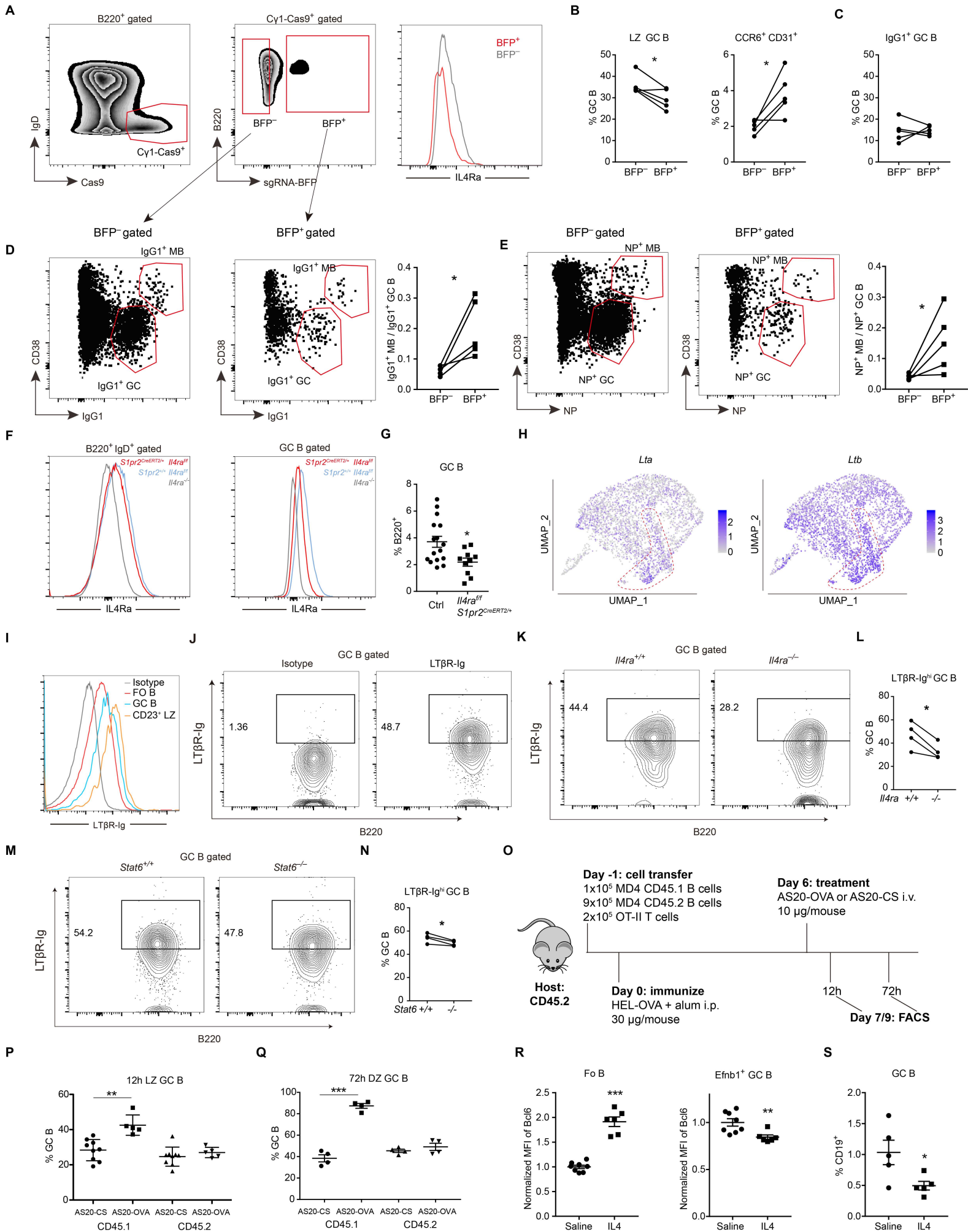


Figure S5. Intrinsic IL4Ra requirement in GC B cells, LT α 1 β 2 expression by CD23⁺ LZ cells, and antigen-loading of GC B cells using AS20-OVA.

(A-E) Conditional knock out *Il4ra* by Cas9-mediated gene targeting. Cas9-GFP expression is driven by *C γ 1^{Cre/+}*. IL4Ra-sgRNA positive cells were marked with BFP. Immunized mice were analyzed on day 14. (A, D, E) Gating strategy and representative FACS profiles of B220⁺ IgD⁻ Cas9-GFP⁺ sgRNA-BFP⁺ or ⁻ cells further gated on CD38⁺ IgG1⁺ memory B cell and CD38⁻ IgG1⁺ GC B cells. Representative histograms of IL4RA in B220⁺ IgD⁻ Cas9-GFP⁺ sgRNA-BFP⁺ or ⁻ cells (A right). Ratio of indicated memory B cell and GC B cell gates shown on right in D and E. (B, C) Frequencies amongst GC B cells (mean \pm SEM) of BFP⁻ and BFP⁺ total LZ cells (B left), CD31⁺CCR6⁺ LZ cells (B right), and IgG1⁺ GC B cells (C) gated as in A. Each symbol represents one mouse. One of two experiments with similar result is shown. **P*<0.05 by paired student's t-test.

(F, G) Control and *S1pr2^{CreERT2/+} Il4ra^{fl/fl}* mice were immunized, treated with tamoxifen and analyzed on day 13. Representative histograms of IL4RA in B220⁺ IgD⁺ follicular B cell and B220⁺ IgD⁻CD38⁻GL7⁺ GC B cells (F). Frequencies (mean \pm SEM) of B220⁺ IgD⁻CD38⁻GL7⁺ GC B cells in B220⁺ B cells (G). Each symbol represents one mouse. Data are pooled from three independent experiments. * *P*<0.05.

(H) UMAP plots of *Lta* and *Ltb* expression in day 7 GC B cell dataset. Color scaled for each gene with log normalized expression level.

(I) Representative histograms of LT α 1 β 2 expression in the B220⁺ FO B cells, the CD95^{hi} GL7^{hi} GC B cells, CD23⁺ CXCR4^{lo} CD86^{hi} LZ GC B cells from B6 mice, determined by staining with LT β R-Ig. Data represent two independent experiments, with at least three mice per experiment.

(J) Representative FACS profiles of $LT\alpha 1\beta 2^+$ detected using $LT\beta R$ -Ig or isotype control in $CD95^{hi} GL7^{hi}$ GC B cells. Data represent one independent experiment with at least three mice per experiment.

(K, L) Mixed 50:50 BM chimeras were made with CD45.1 wild-type ($Il4ra^{+/+}$) and CD45.2 $Il4ra^{-/-}$ BM cells. Representative FACS profiles (K) and frequencies of $LT\alpha 1\beta 2^+$ cells in $CD95^{hi} GL7^{hi}$ GC B cells (L) with indicated genotypes in chimeras. Each symbol represents one mouse, and each line represents the same mouse. * $P < 0.05$.

(M, N) Mixed 50:50 BM chimeras were made with CD45.1 wild-type ($Stat6^{+/+}$) and CD45.2 $Stat6^{-/-}$ BM cells. Representative FACS profiles (M) and frequencies of $LT\alpha 1\beta 2^+$ cells in $CD95^{hi} GL7^{hi}$ GC B cells (N) with indicated genotypes in chimeras. Each symbol represents one mouse, and each line represents the same mouse. * $P < 0.05$.

(O-Q) AS20-OVA stimulation scheme diagram (O). Frequencies (mean \pm SEM) of LZ B cells in GC 12h post indicated treatment (P) or DZ B cells in GC 72h post treatment (Q). Each symbol represents one mouse.

(R) Immunized mice received IL4- α IL4 complex or saline intravenously once per day on day 11, 12, 13 post immunization and were analyzed on day 14. Normalized geometric mean fluorescence intensity (MFI) of Bcl6 in $CD19^+ IgD^+$ follicular B cells (R left) and $CD19^+ IgD^- Fas^{hi} GL7^{hi} Efnb1^+$ mature GC B cells. ** $P < 0.01$, *** $P < 0.001$.

(S) Immunized mice received IL4- α IL4 complex or saline intravenously once per day on day 10, 11, 12, 13 post immunization and were analyzed on day 14. Frequencies (mean \pm SEM) of $CD95^{hi} GL7^{hi}$ GC B cells in $CD19^+$ B cells.

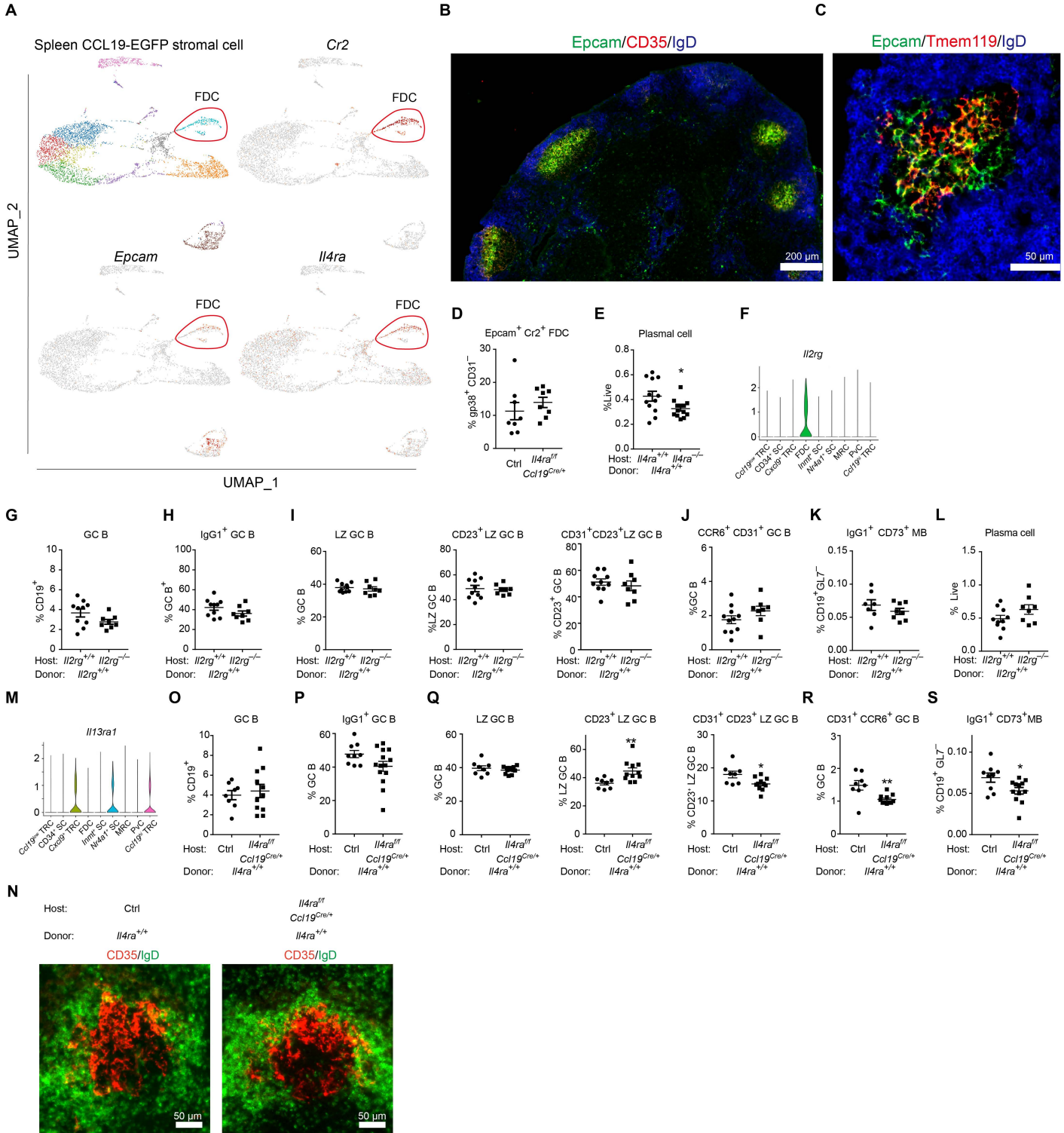


Figure S6, Related to Figure 6. IL4RA and EPCAM are expressed by the FDCs in spleen and LNs.

(A) Expression of *Cr2*, *Ii4ra*, and *Epcam* projected on UMAP plots. Data are from the published dataset (Cheng et al., 2019).

(B) Representative FDC image in mesenteric LNs co-stained with EPCAM, CD35 and IgD. Sections are representative of multiple LNs from 3 mice. Scale bar, 200 μ m.

(C) Representative FDC image in mesenteric LNs co-stained with EPCAM, Tmem119 and IgD. Sections are representative of multiple LNs from 3 mice. Scale bar, 50 μ m.

(D) Frequencies (mean \pm SEM) of CR2⁺ Epcam⁺ FDC in CD45⁻ CD31⁻ gp38⁺ stromal cell 13 days after immunization in mice with indicated genotypes. Each symbol represents one mouse. Data are pooled from two independent experiments.

(E) Frequencies (mean \pm SEM) of IgD^{low} CD138^{hi} plasma cell in splenocytes 13 days after immunization in reversed chimeras. Each symbol represents one mouse. Data are pooled from three independent experiments. * $P < 0.05$.

(F) Violin plots of expression of *Ii2rg* in different stromal cell subsets.

(G-L) Reverse chimaeras were made by reconstituting irradiated *Ii2rg*^{+/+} and *Ii2rg*^{-/-} mice with wild-type (*Ii2rg*^{+/+}) BM. Frequencies (mean \pm SEM) of CD95^{hi} GL7^{hi} GC B cells in CD19⁺ B cells (G), IgG1⁺ cells in GC B cells (H), LZ cells in GC B cells (I left), CD23⁺ cells in LZ GC B cells (I middle), CD31⁺ cells in CD23⁺ LZ GC B cells (I right) and CCR6⁺ CD31⁺ cells (J) in GC B cells 13 days after immunization. (K) Frequencies (mean \pm SEM) of IgG1⁺ CD73⁺ memory cells in CD19⁺ GL7⁻ non-GC B cells. (L) Frequencies (mean \pm SEM) of IgD^{low} CD138^{hi} plasma cell in splenocytes. Each symbol represents one mouse. Data are pooled from two independent experiments.

(M) Violin plots of expression of *Ii13ra1* in different stromal cell subsets.

(N-S) Reverse chimaeras were made by reconstituting irradiated *I14ra*^{+/+} and *Ccl19*^{Cre/+} *I14ra*^{fl/fl} mice with wild-type (*I14ra*^{+/+}) BM. Representative FDC images in the spleen co-stained with CD35 and IgD. Sections are representative of multiple spleens from 3 mice. Scale bar, 50 μ m (N). Frequencies (mean \pm SEM) of CD95^{hi} GL7^{hi} GC B cells in CD19⁺ B cells (O), IgG1⁺ cells in the GC B cells (P), CXCR4^{lo} CD86^{hi} LZ cells in GC B cells (Q left), CD23⁺ cells in LZ GC B cells (Q middle), CD31⁺ cells in CD23⁺ LZ GC B cells (Q right), and CD31⁺CCR6⁺ cells in the GC B cells (R), and CD73⁺ IgG1⁺ memory B cell in CD19⁺GL7⁻ B cells (S) 13 days after NP-KLH immunization. Each symbol represents one mouse. Data are pooled from three independent experiments. ** $P < 0.01$, * $P < 0.05$.

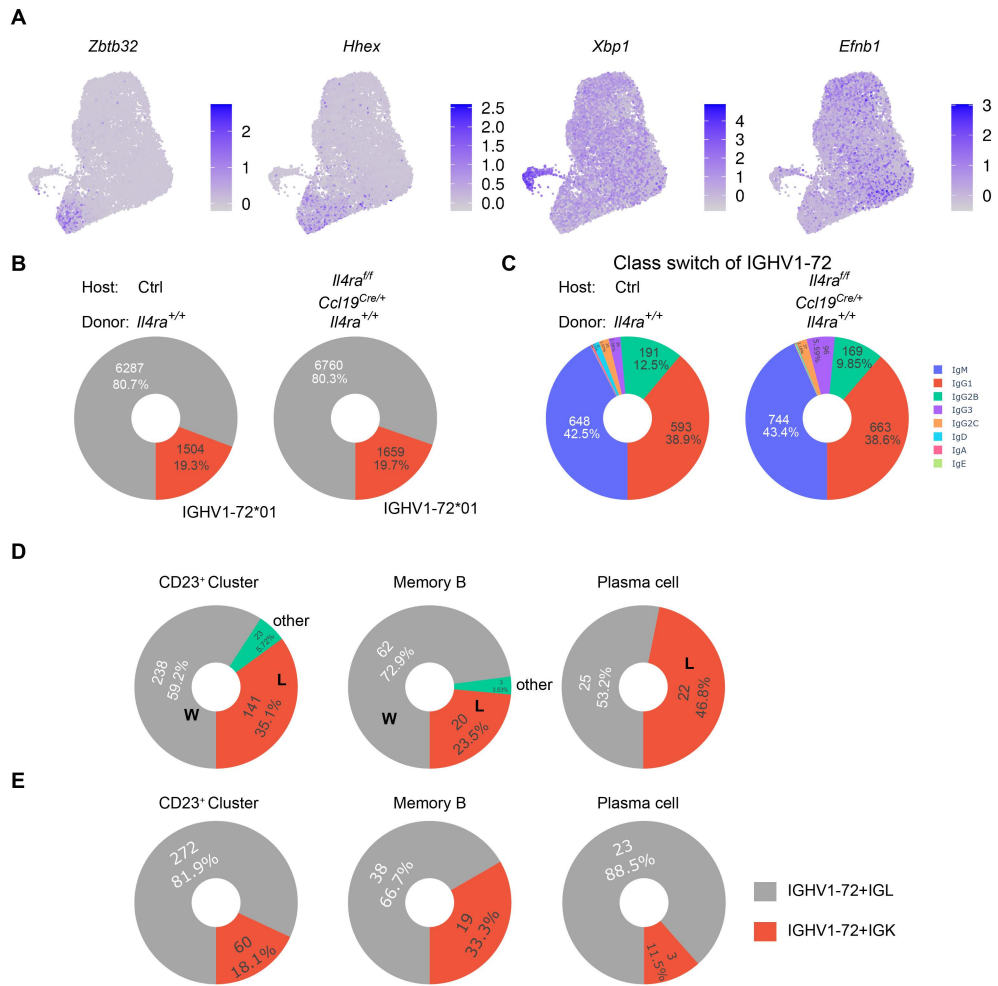


Figure S7, Related to Figure 7. scVDJ analysis of stroma cell IL4Ra-deficient mice.

(A-E) Reverse chimaeras were made by reconstituting irradiate *Il4ra*^{+/+} and *Ccl19*^{Cre/+} *Il4ra*^{fl/fl} mice with wild-type (*Il4ra*^{+/+}) BM. Single cell RNA sequencing and single cell V(D)J sequencing was performed on B220⁺ CD95^{hi} GL7^{hi} IgD⁻ cells sorted 14 post-immunization. Contaminating naïve B cells and non-B cells were filtered during the data analysis.

(A) UMAP plots of the expression of memory B cell markers (*Zbtb32* and *Hhex*), plasma cell marker (*Xbp1*), and GC B cell marker (*Efnb1*). Color scaled for each gene with log normalized expression level.

(B) Pie chart shows the usage of IGHV1-72*01 in different conditions.

(C) Pie chart shows the immunoglobulin isotypes of IGHV1-72*01 in different conditions.

(D) Pie chart shows the W33L mutation in different cell types. Control and stoma IL4Ra-deficient samples were pooled together.

(E) Pie chart shows the IGHV1-72*01 coupled light chain frequency in different cell types. Control and stoma IL4Ra-deficient samples were pooled together.